Published in final edited form as:
J Orthop Res. 2013 March ; 31(3): 350–356. doi:10.1002/jor.22237.

Ift88 regulates Hedgehog signaling, *Sfrp5* expression, and β-catenin activity in post-natal growth plate

Ching-Fang Chang and **Rosa Serra***
Department of Cell Biology, University of Alabama at Birmingham, Birmingham, AL

Abstract

Primary cilia are present on most cell types including chondrocytes. Dysfunction of primary cilia results in pleiotropic symptoms including skeletal dysplasia. Previously, we showed that deletion of *Ift88* and subsequent depletion of primary cilia from chondrocytes resulted in disorganized columnar structure and early loss of growth plate. To understand underlying mechanisms whereby Ift88 regulates growth plate function, we compared gene expression profiles in normal and *Ift88* deleted growth plates. Pathway analysis indicated that Hedgehog (Hh) signaling was the most affected pathway in mutant growth plate. Expression of the Wnt antagonist, *Sfrp5,* was also down-regulated. In addition, *Sfrp5* was up-regulated by Shh in rib chondrocytes and regulation of *Sfrp5* by Shh was attenuated in mutant cells. This result suggests *Sfrp5* is a downstream target of Hh and that Ift88 regulates its expression. Sfrp5 is an extracellular antagonist of Wnt signaling. We observed an increase in Wnt/β-catenin signaling specifically in flat columnar cells of the growth plate in *Ift88* mutant mice as measured by increased expression of Axin2 and Lef1 as well as increased nuclear localization of β-catenin. We propose that Ift88 and primary cilia regulate expression of Sfrp5 and Wnt signaling pathways in growth plate via regulation of Ihh signaling.

Keywords

primary cilia; Ift88; Hedgehog; Sfrp5; Wnt

Introduction

Primary cilia are nonmotile microtubule-based organelles present on almost every type of cell (1). The ciliary body is comprised of microtubule bundles elongating from one of the centrioles (basal body), covered by a specialized plasma membrane. Primary cilia are built up and maintained by a process called intraflagellar transport (IFT), in which IFT proteins associate with kinesin motors or dyneins to carry cargos into or out of primary cilia, respectively. Deletion of IFTs or motor proteins (e.g. Ift88 and Kif3a) results in depletion of primary cilia (2). Extensive studies in the past ten years have demonstrated that primary cilia act as the hub for several signaling pathways, including Hedgehog (Hh), Wnt, Platelet Derived Growth Factor, and fluid flow (3). Dysfunction of primary cilia is associated with a group of genetic diseases called ciliopathies, characterized by pleiotropic symptoms including skeletal dysplasias (4).

The role of primary cilia in skeletal development has been shown in studies using mouse models (5). In our previous study, we generated *Col2aCre;Kif3a*$^{fl/fl}$ and *Col2aCre;Ift88*$^{fl/fl}$

*Corresponding author: Rosa Serra, Ph.D., Department of Cell Biology, University of Alabama at Birmingham, 1918 University Blvd., 660 MCLM, Birmingham, AL 35294-0005, 205-934-0842, rserra@uab.edu.

None of the authors have any conflicts to declare.

mice in which primary cilia were specifically deleted in chondrocytes. The mutant mice showed postnatal cartilage phenotypes including disorganization of columnar structure and accelerated hypertrophic differentiation resulting in complete loss of growth plate around two-weeks of age (6). These mice also developed symptoms of early osteoarthritis (7).

Longitudinal bone growth results from the complex events of chondrocyte differentiation in the growth plate. Chondrocytes in the resting zone are stem-like, round-shaped cells that serve as a reservoir to generate proliferating chondrocytes. In the proliferative zone, cells are flat and arranged into a columnar structure. It has been suggested that the columnar structure is a result of a process called chondrocyte rotation. During this process, chondrocytes divide perpendicular to the long axis of the bone then migrate one on top of the other to form columns of cells (8). In addition to primary cilia (6), integrins (9), Hh (10), and Wnt/ PCP signaling (11) have been implicated in regulation of chondrocyte rotation. When the proliferating cells in the growth plate stop dividing they undergo hypertrophic differentiation. The Indian hedgehog (Ihh)/ Parathyroid Hormone-related Protein (PTHrP) feedback loop is a key regulator of hypertrophic differentiation (12). Ihh, a secreted ligand produced by prehypertrophic chondrocytes, stimulates perichondrial cells and periarticular chondrocytes to synthesize PTHrP, which acts on receptor expressing cells in the growth plate to delay hypertrophic differentiation. Wnt/ β-catenin signaling has also been shown to regulate hypertrophic differentiation and mice with activated β-catenin demonstrate premature closure of the growth plate in post-natal mice (13; 14).

In this study, we used microdissection and microarray technology to characterize global changes in gene expression in control and *Ift88* depleted growth plates. We focused specifically on the columnar cells in the growth plate at postnatal day 7, when alterations in the *Ift88* mutant growth plate were just beginning to be seen. We identified a list of genes whose expression was altered in mutant versus control growth plates. Altered expression was verified by real time RT- PCR for a subset of genes. Pathway analysis indicated that down-regulation of Hh signaling was the most significant alteration. Down-regulation of *Sfrp5* was also observed in mutant cartilage. Sfrp5 is an extracelluar antagonist of Wnt signaling pathways (15; 16). We then demonstrated that Shh directly regulates *Sfrp5* expression and that this regulation is dependent on Ift88. An increase in Wnt/β-catenin signaling was observed specifically in the flat columnar cells in mutant growth plates. We propose that Sfrp5, acting down-stream of Ift88 and Ihh signaling, at least partially regulates growth plate phenotype through regulation of Wnt signaling pathways.

Materials and Methods

Animals

All animal procedures were approved by the Institutional Animal Care and Use Committee (IACUC) of the University of Alabama at Birmingham. *Ift88*$^{fl/fl}$ mice were a gift from Dr. Bradley Yoder, University of Alabama at Birmingham, (17) *Col2aCre* mice were obtained from Jackson labs (stock No. 003554), (18). No haploinsufficiency was observed at the level of Ift88 protein expression or phenotype (data not shown); therefore, *Col2aCre;Ift88*$^{fl/wt}$ or *Ift88*$^{fl/fl}$ littermates were used as controls to compare with *Col2aCre;Ift88*$^{fl/fl}$ mutants.

Tissue preparation and RNA extraction

Cryosections with thickness of 40 mm were used. Slides were dehydrated in an ethanol series followed by xylene. Slides were air-dried before micro-dissection. Proliferating zone chondrocytes were cut out from proximal tibia and distal femur using an 18 gauge needle. RNA was isolated using the RNAqueous®-Micro Kit (Ambion, AM1931). Thirty-five

sections from a combination of tibia and femur growth plates from each mouse were used for the RNA isolation.

Affymetrix microarrays

The Gene Expression Shared Facility, Heflin Center for Genomic Sciences at the University of Alabama, Birmingham performed the microarrays. Affymetrix Mouse 430 2.0 GeneChip Array was used. The quality of each RNA sample was determined using a 2100 Agilent Bioanalyzer prior to RNA labeling. Detailed procedures are presented in the manufacturer's GeneChip Expression Technical Manual (Affymetrix). Gene expression levels were extracted using AGCC (Affymetrix GeneChip Command Console).

Microarray analysis

Statistical analysis and gene lists for the array experiments were generated using the software package GeneSprings (Agilent, Santa Clara, CA). Gene lists were generated from the raw GeneChip files (.cel) using the default settings. The wild type group was used as a baseline to calculate the intensity ratio/fold changes of the mutant versus the wild type groups. The p-values were obtained by unpaired T-test assuming unequal variance. Pathway analysis was done using Ingenuity Pathway Analysis (Redwood City, CA). Microarray data was deposited into the Gene Expression Omnibus (GEO; accession number GSE35003).

Costal chondrocyte culture

Chondrocytes were isolated from rib cages of mice that were less than 3 days old and cultured according to standard protocols (19). Cells were plated at a density of $2*10^5$ cells/cm^2. Culture medium contained DMEM/F12, 1 mM sodium pyruvate, 2 mM L-glutamine, 50 ug/mL L-ascorbate-2-phosphate (Fluka), 50 U penicillin, and 50 mg streptomycin.

Real-time RT-PCR

RNA was isolated from microdissected growth plate using the Ambion kit. For costal chondrocytes, RNA was extracted using Trizol reagent, (Invitrogen). RNA samples were DNaseI treated and real time RT-PCR was performed using the QuantiFast® SYBR Green RT-PCR kit (Qiagen) and LightCycler® 480 (Roche). Data was analyzed with REST 2009 software (www.qiagen.com/Products/REST2009Software.aspx?r=8042); (20). Reference genes were selected that were not regulated by treatment and expressed at a similar level to the test genes (www.qiagen.com/products/pcr/quantitect/housekeepinggenes.aspx). Beta-2-microglobulin (B2m) was used when assaying tissue and Hypoxanthine guanine phosphoribosyl transferase (Hprt) was used for cell culture experiments.

Immunostaining

Ten micron cryosections were fixed in ice-cold methanol and washed with PBS. Mouse anti-γ-tubulin antibody (Sigma, T6557), rabbit anti-Arl13b (a gift from Dr. Tamara Caspary, Emory University (21)), biotinylated anti-mouse IgG, biotinylated anti-rabbit IgG, Alexa488 conjugated or Cy3-conjugated streptavidin were used to stain for cilia. M.O.M blocking reagent (Vector Laboratories) was used. Polyclonal anti-β-catenin antibody (Cell signaling) was used to localize β-cateinin in tissue sections. For staining of primary cilia on cultured chondrocytes, mouse anti-acetylated tubulin (Sigma T6793) and rabbit anti-γ-tubulin (Sigma T3559) antibodies were used. Avidin/Biotin blocking kit (Vector Labs) was used before staining of the second antibody.

Results

Gene expression is altered in primary cilia depleted columnar growth plate chondrocytes

To begin to understand how *Ift88* and depletion of primary cilia in the growth plate affects growth plate function, we compared gene expression in control and *Col2aCre;Ift88*$^{fl/fl}$ chondrocytes using Affymetrix gene arrays. First, depletion of primary cilia in the growth plate was verified by immunostaining to Arl13b, a cilia specific protein (21); (Fig. 1A and B). Next, the flat columnar cells of the of the growth plate was microdissected from thick sections of post-natal day 7 (P7) proximal tibiae and distal femur from control and mutant mice. This is the time the abnormalities in the growth plate first start and the columnar structure of the growth plate can be easily seen under a dissecting microscope (Fig. 1C and D). RNA was isolated from the dissected tissue and quality control tested. The high quality RNA from two controls and two mutants was amplified, labeled, and then hybridized each to separate Affymetrix Mouse 430 2.0 GeneChip Arrays. Microarray results were analyzed using GeneSpring software. A total of 48 genes showed at least a two-fold change of expression (up or down) in mutant columnar growth plate chondrocytes compared to controls (T-test, $p<0.05$), with 28 genes down-regulated (Table 1) and 20 genes up-regulated (Table 2). The change in expression of selected genes was verified by real time RT-PCR (Table 3) using separate RNA samples isolated from 3 control and 3 mutant mice. Combined PCR data from the three biological replicates was analyzed using REST software, which normalizes results and calculates the relative fold difference in gene expression, standard error (65% confidence interval), and statistical significance across experiments (20). The change in expression for all of the selected genes was consistent with the microarray result (Table 3). Pathway analysis using Ingenuity Pathway Analysis software indicated that Hh signaling was significantly down-regulated in the mutant cells relative to controls (p-value= 0.002). This was evident by down-regulation of and *Gli1* and *Ptch1*, targets of Hh signaling. Cell death and cell growth pathways were also regulated (p-values range = $9.38 \text{ X } 10^{-5}$ – $3.17 \text{ X } 10^{-2}$ and $9.52 \text{ X } 10^{-5}$ – $2.77 \text{ X } 10^{-2}$). We had previously reported that loss of cilia in the growth plate resulted in reduced chondrocyte proliferation and accelerated hypertrophic differentiation. Alterations in apoptosis as measured by TUNEL staining, which measures late stages of apoptosis, were not previously detected in *Kif3a* or *Ift88* mutants (6). Down-regulation of *Prelp*, a glycosaminoglycan and collagen-binding anchor protein that is highly expressed in columnar growth plate chondrocytes (22), in mutant chondrocytes suggests that the extracellular matrix environment at P7 was already changing even though only minor differences in growth plate histology were observed. The results indicate that deletion of *Ift88* in proliferating zone chondrocytes results in changes in gene expression that may provide clues about the mechanism of Ift88 and cilia function in growth plate chondrocytes.

Sfrp5 is down-regulated in cilia depleted growth plate and canonical signaling is up-regulated

Two proteins that modulate Wnt signaling, Secreted Frizzled-related Proteins −5 and −2 (Sfrp5 and Sfrp2), were down-regulated and up-regulated, respectively, in mutant chondrocytes compared to controls (Tables 1–3) (15; 16). Sfrp5 is expressed in proliferating chondrocytes in the growth plate while Sfrp2 is more highly expressed in the developing joint and perichondrium (23). Since inappropriate activation of Wnt/β-catenin signaling promotes hypertrophic differentiation and induces premature closure of the growth plate (13; 14) similar to what is seen in the *Ift88*-deleted mice, we tested whether low levels of Sfrp5 in *Ift88* mutants correlated with increased canonical Wnt signaling. Wnt/β-catenin signaling was measured as nuclear localization of β-catenin, and expression of *Axin2* and *Lef1*, down-stream targets of β-catenin, in mutant and control growth plates (Fig. 2). Real time RT-PCR using RNA isolated from microdissected columnar growth plate chondrocytes indicated a small but significant up-regulation of both *Axin2* and *Lef1* (Figure 2A). In sections from P7

control limbs, β-catenin was strongly detected by immunoflourescence in the nucleus of resting and maturing prehypertrophic cells immediately adjacent to the hypertrophic zone. Few flat, columnar cells in the growth plate demonstrated nuclear β-catenin staining, similar to what has been previously reported (Fig. 2 B, D) (24). A similar staining pattern was observed in the resting and prehypertrophic cells in the *Col2aCre;Ift88*$^{fl/fl}$ limbs (Fig. 2C); however, there was an increase in nuclear β-catenin staining specifically in the flat columnar cells of the growth plate (Figure 2C, E) and the increase was statistically significant (Fig. 2F). We conclude that Wnt/β-catenin signaling is increased in the columnar cells of *Ift88*-deleted growth plate when *Sfrp5* is reduced.

Sfrp5 is a downstream target of Hh signaling

Since Hh was the most significantly affected signaling pathway in *Ift88*-deleted chondrocytes and it has been shown that loss of Ihh signaling in post-natal growth plate has similar phenotype to the *Ift88*-deleted mice (10; 25), we tested the hypothesis that Hh signaling regulates Sfrp5. Costal chondrocytes from newborn control and *Col2aCre;Ift88*$^{fl/fl}$ mice were isolated, placed in culture and treated with 0.5μg recombinant Shh-N protein/ ml for varying times (Fig. 3). RNA was isolated and used in real time RT-PCR to determine the relative expression levels of *Gli1*, a known target of Hh signaling, and *Sfrp5*. First, we confirmed using immunofluorescent staining that cilia were depleted in *Ift88*-deleted cells grown in culture (Fig. 3A, B) and by western blot that Ift88 protein was down-regulated (Fig. 3C). We then showed that, as expected, *Gli1* and *Sfrp5* were down-regulated in untreated mutant cells relative to controls (Fig. 3D, E). When control cells were treated with Shh-N protein, *Gli1* was significantly up-regulated by 8 hours with highest up-regulation by 24 hours (Fig. 3D, F). *Sfrp5* was significantly up regulated by 16 hours with the highest expression at 24 hours after treatment (Fig. 3D, F). In contrast, in mutant cells, up-regulation of *Gli1* and *Sfrp5* by Shh treatment was delayed and attenuated (Fig. 3D, F). Significant changes in gene expression were not detected in mutant cells until 24 hours and the level of induction was reduced relative to control cells. The response to Shh in mutant cells at 24 hours could result from a few cells that may retain cilia in the cultures. The results suggest that *Sfrp5* is a downstream target of Hh signaling and that down-regulation of Sfrp5 in *Ift88*-deleted growth plate is likely due to regulation of Hh signaling by primary cilia. Two putative Gli binding sites (26) were identified in the *Sfrp5* promoter region supporting this hypothesis (supplemental Fig. 1). This is the first report showing that *Sfrp5* is regulated by Hh.

Discussion

To understand the mechanisms of cilia action in the growth plate, we compared gene expression patterns in control and *Col2aCre;Ift88*$^{fl/fl}$ growth plates. The RNA samples used were prepared from micro-dissected columnar growth plate chondrocytes at postnatal day 7 when alterations in histology were just beginning. Analysis using micro-dissected tissue sections avoids contamination from surrounding cells, which could mask changes in gene expression in a specific cell type. Previously, we reported that Hh signaling was not altered at P10 in growth plate from *Col2aCre;Kif3a*$^{fl/fl}$ mice because we did not detect changes in *Ptch1* expression by semi-quantitative RT-PCR using samples isolated from total metaphysis and epiphysis (6). While this may indicate some molecular differences in how Kif3a and Ift88 function, it is more likely due to how the experiments were done. In this study, with samples isolated specifically from columnar growth plate chondrocytes, we found that Hh signaling was significantly affected. This result fits well with the current model that primary cilia are required for ligand-dependent Hh signaling (3).

The importance of primary cilia in Hh signaling has been demonstrated by several studies. Primary cilia are required for ligand-dependent activation of Hh signaling and ligand-

independent proteolytic processing of full length Gli3 activator to repressor (5). Without primary cilia, both ligand-mediated activation and Gli3-mediated repression of Hh signaling are disrupted. Depending on whether Gli activator or repressor functions are dominant, loss of primary cilia has varying effects on different tissues. Here we show that ligand-dependent Hh signaling is disrupted in postnatal *Col2aCre;Ift88*$^{fl/fl}$ growth plate as evidenced by reduced expression of *Ptc1* and *Gli1* mRNA. In addition, the response to Shh in cilia-depleted costal chondrocytes in culture is attenuated. Mice with a conditional deletion of Ihh in the postnatal growth plate, *Col2aCreER;Ihh*$^{fl/fl}$, have a similar phenotype to *Col2aCre;Ift88*$^{fl/fl}$ mice including accelerated hypertrophic differentiation and disorganization of the columnar structure of the growth plate (25). These results together suggest that ligand-dependent Gli activator function is dominant in the post-natal growth plate and Ift88 is required for activator functions. In contrast, we recently showed that deletion of *Ift88* in articular cartilage results in up-regulation of Hh signaling, reduced Gli3 repressor to activator ratio, and symptoms of early osteoarthritis (7). Up-regulation of Hh signaling has been associated with osteoarthritis in human patients and mouse models of osteoarthritis (27). In embryonic growth plate, Hh inhibits hypertrophic differentiation though regulation of PTHrP expression. In contrast, in articular cartilage, a PTHrP-independent pathway becomes dominant and Hh signaling promotes chondrocyte hypertrophy (28). Therefore, low levels of Hh signaling are required in articular cartilage where Gli3 repressor function is dominant. The results fit well with what is known about the molecular differences between articular and growth plate cartilage and point to a role for Ift88 in this regulation.

In this study, we identified *Sfrp5* as a downstream target of cilia and Hh signaling in the growth plate. The *Sfrp* gene family contains five members that are classified into *Sfrp1* and *Frzb* subfamilies. *Sfrp1/2/5* belong to the *Sfrp1* subfamily (29). In embryonic cartilage development, *Sfrp2* is expressed in synovial joints and *Sfrp5* is expressed in proliferating chondrocytes (23). In our study, *Sfrp2* was up-regulated and *Sfrp5* was down-regulated in Ift88 deficient growth plate. *Sfrp5* was up-regulated by Hh in chondrocytes in culture while *Sfrp2* expression was not altered in *Ift88*-deleted costal chondrocytes nor was Sfrp2 regulated by Shh (not shown). Mice with activated β-catenin demonstrate accelerated hypertrophic differentiation and premature closure of the growth plate (13; 14). Deletion of Sfrp1, the Sfrp with the highest homology to Sfrp5, in mice also resulted in accelerated hypertrophic differentiation and activation of Wnt/β-catenin signaling in the growth plate similar to what we see in the *Ift88*-deleted mice (30). We hypothesize that Ihh regulates Sfrp5 expression through Ift88/ primary cilia and that Sfrp5 regulates Wnt/β-catenin activity, hypertrophic differentiation, and premature closure of the growth plate. The idea that Wnt signaling is regulated indirectly by Ift88/ cilia through Hh signals could explain some of the conflicting results regarding whether or not β-catenin signaling is regulated by primary cilia (3).

Deletion of *Ift88* and disruption of Hh signaling in growth plate both also result in disorganized columnar structure in the growth plate (6; 25) but the mechanism of how these signals regulate chondrocyte orientation is not clear. The method to generate columnar structure in the growth plate was first proposed by Dodds in 1930 (8) based on microscopic observations of tissue sections. Proliferating chondrocytes divide perpendicularly to the axis of long bone, then migrate one on the top of another. This process, called chondrocytes rotation, is similar to the convergent extension movements that take place during embryonic gastrulation (31). Wnt/PCP signaling is a key regulator for this process (32) and it was recently shown that chondrocyte rotation is regulated by Wnt/PCP signaling (11). Sfrps genetically interact with the core PCP component *Vangl2* (16), and function redundantly in regulation of canonical Wnt/β-catenin and noncanonical Wnt/PCP signaling (16). It has been suggested that primary cilia restrain canonical Wnt/β-catenin signaling and act as a

molecular switch between canonical Wnt and noncanonical Wnt/PCP signaling ((33). Since the Wnt/ PCP pathway and Ihh regulate organization of the growth plate (11), we speculate that in addition to regulating Wnt/βcatenin signaling and hypertrophic differentiation, Sfrp5 acts downstream of Ihh to regulate organization of the growth plate through PCP. Sfrp5 may be a molecular switch between Wnt signaling in the context of growth plate. At this time, there are no good down-stream markers of PCP signaling in the growth plate to test this hypothesis directly.

Supplementary Material

Refer to Web version on PubMed Central for supplementary material.

Acknowledgments

We would like to thank Drs. Michael Crowley and David Crossman at the Heflin Center for Genetics, University of Alabama at Birmingham, for help with the microarray and data analysis. We also thank Dr. Bradley Yoder, Department of Cell Biology, University of Alabama at Birmingham, for providing the *Ift88*$^{fl/fl}$ mice. Funding for this study was through NIH grants AR055110 and AR053860 to RS.

References

1. Ishikawa H, Marshall WF. Ciliogenesis: Building the cell's antenna. Nat Rev Mol Cell Biol. 2011; 12:222–234. [PubMed: 21427764]
2. Marshall WF. Basal bodies platforms for building cilia. Curr Top Dev Biol. 2008; 85:1–22. [PubMed: 19147000]
3. Goetz SC, Anderson KV. The primary cilium: A signalling centre during vertebrate development. Nat Rev Genet. 2010; 11:331–344. [PubMed: 20395968]
4. Sharma N, Berbari NF, Yoder BK. Ciliary dysfunction in developmental abnormalities and diseases. Curr Top Dev Biol. 2008; 85:371–427. [PubMed: 19147012]
5. Haycraft CJ, Serra R. Cilia involvement in patterning and maintenance of the skeleton. Curr Top Dev Biol. 2008; 85:303–332. [PubMed: 19147010]
6. Song B, Haycraft CJ, Seo HS, et al. Development of the post-natal growth plate requires intraflagellar transport proteins. Dev Biol. 2007; 305:202–216. [PubMed: 17359961]
7. Chang CF, Ramaswamy G, Serra R. Depletion of primary cilia in articular chondrocytes results in reduced gli3 repressor to activator ratio, increased hedgehog signaling, and symptoms of early osteoarthritis. Bone. 2012
8. Dodds GS. Row formation and other types of arrangement of cartilage cells in endochondral ossifcation. Anat Rec. 1930; 46:385–399.
9. Aszodi A, Hunziker EB, Brakebusch C, Fassler R. Beta1 integrins regulate chondrocyte rotation, g1 progression, and cytokinesis. Genes Dev. 2003; 17:2465–2479. [PubMed: 14522949]
10. St-Jacques B, Hammerschmidt M, McMahon AP. Indian hedgehog signaling regulates proliferation and differentiation of chondrocytes and is essential for bone formation. Genes Dev. 1999; 13:2072–2086. [PubMed: 10465785]
11. Li Y, Dudley AT. Noncanonical frizzled signaling regulates cell polarity of growth plate chondrocytes. Development. 2009; 136:1083–1092. [PubMed: 19224985]
12. Kronenberg HM. Developmental regulation of the growth plate. Nature. 2003; 423:332–336. [PubMed: 12748651]
13. Yuasa T, Kondo N, Yasuhara R, et al. Transient activation of wnt/{beta}-catenin signaling induces abnormal growth plate closure and articular cartilage thickening in postnatal mice. Am J Pathol. 2009; 175:1993–2003. [PubMed: 19815716]
14. Tamamura Y, Otani T, Kanatani N, et al. Developmental regulation of wnt/beta-catenin signals is required for growth plate assembly, cartilage integrity, and endochondral ossification. J Biol Chem. 2005; 280:19185–19195. [PubMed: 15760903]

15. Li Y, Rankin SA, Sinner D, et al. Sfrp5 coordinates foregut specification and morphogenesis by antagonizing both canonical and noncanonical wnt11 signaling. Genes Dev. 2008; 22:3050–3063. [PubMed: 18981481]
16. Satoh W, Matsuyama M, Takemura H, et al. Sfrp1, sfrp2, and sfrp5 regulate the wnt/beta-catenin and the planar cell polarity pathways during early trunk formation in mouse. Genesis. 2008; 46:92–103. [PubMed: 18257070]
17. Haycraft CJ, Zhang Q, Song B, et al. Intraflagellar transport is essential for endochondral bone formation. Development. 2007; 134:307–316. [PubMed: 17166921]
18. Ovchinnikov DA, Deng JM, Ogunrinu G, Behringer RR. Col2a1-directed expression of cre recombinase in differentiating chondrocytes in transgenic mice. Genesis. 2000; 26:145–146. [PubMed: 10686612]
19. Thirion S, Berenbaum F. Culture and phenotyping of chondrocytes in primary culture. Methods Mol Med. 2004; 100:1–14. [PubMed: 15280583]
20. Pfaffl MW, Horgan GW, Dempfle L. Relative expression software tool (rest) for group-wise comparison and statistical analysis of relative expression results in real-time pcr. Nucleic Acids Res. 2002; 30:e36. [PubMed: 11972351]
21. Caspary T, Larkins CE, Anderson KV. The graded response to sonic hedgehog depends on cilia architecture. Dev Cell. 2007; 12:767–778. [PubMed: 17488627]
22. Grover J, Roughley PJ. Characterization and expression of murine prelp. Matrix Biol. 2001; 20:555–564. [PubMed: 11731272]
23. Witte F, Dokas J, Neuendorf F, et al. Comprehensive expression analysis of all wnt genes and their major secreted antagonists during mouse limb development and cartilage differentiation. Gene Expr Patterns. 2009; 9:215–223. [PubMed: 19185060]
24. Hens JR, Wilson KM, Dann P, et al. Topgal mice show that the canonical wnt signaling pathway is active during bone development and growth and is activated by mechanical loading in vitro. J Bone Miner Res. 2005; 20:1103–1113. [PubMed: 15940363]
25. Maeda Y, Nakamura E, Nguyen MT, et al. Indian hedgehog produced by postnatal chondrocytes is essential for maintaining a growth plate and trabecular bone. Proc Natl Acad Sci U S A. 2007; 104:6382–6387. [PubMed: 17409191]
26. Sasaki H, Hui C, Nakafuku M, Kondoh H. A binding site for gli proteins is essential for hnf-3beta floor plate enhancer activity in transgenics and can respond to shh in vitro. Development. 1997; 124:1313–1322. [PubMed: 9118802]
27. Lin AC, Seeto BL, Bartoszko JM, et al. Modulating hedgehog signaling can attenuate the severity of osteoarthritis. Nat Med. 2009; 15:1421–1425. [PubMed: 19915594]
28. Mak KK, Kronenberg HM, Chuang PT, et al. Indian hedgehog signals independently of pthrp to promote chondrocyte hypertrophy. Development. 2008; 135:1947–1956. [PubMed: 18434416]
29. Bovolenta P, Esteve P, Ruiz JM, et al. Beyond wnt inhibition: New functions of secreted frizzled-related proteins in development and disease. J Cell Sci. 2008; 121:737–746. [PubMed: 18322270]
30. Gaur T, Rich L, Lengner CJ, et al. Secreted frizzled related protein 1 regulates wnt signaling for bmp2 induced chondrocyte differentiation. J Cell Physiol. 2006; 208:87–96. [PubMed: 16575902]
31. Wallingford JB, Fraser SE, Harland RM. Convergent extension: The molecular control of polarized cell movement during embryonic development. Dev Cell. 2002; 2:695–706. [PubMed: 12062082]
32. Kiefer JC. Planar cell polarity: Heading in the right direction. Dev Dyn. 2005; 233:695–700. [PubMed: 15778996]
33. He X. Cilia put a brake on wnt signalling. Nat Cell Biol. 2008; 10:11–13. [PubMed: 18172427]

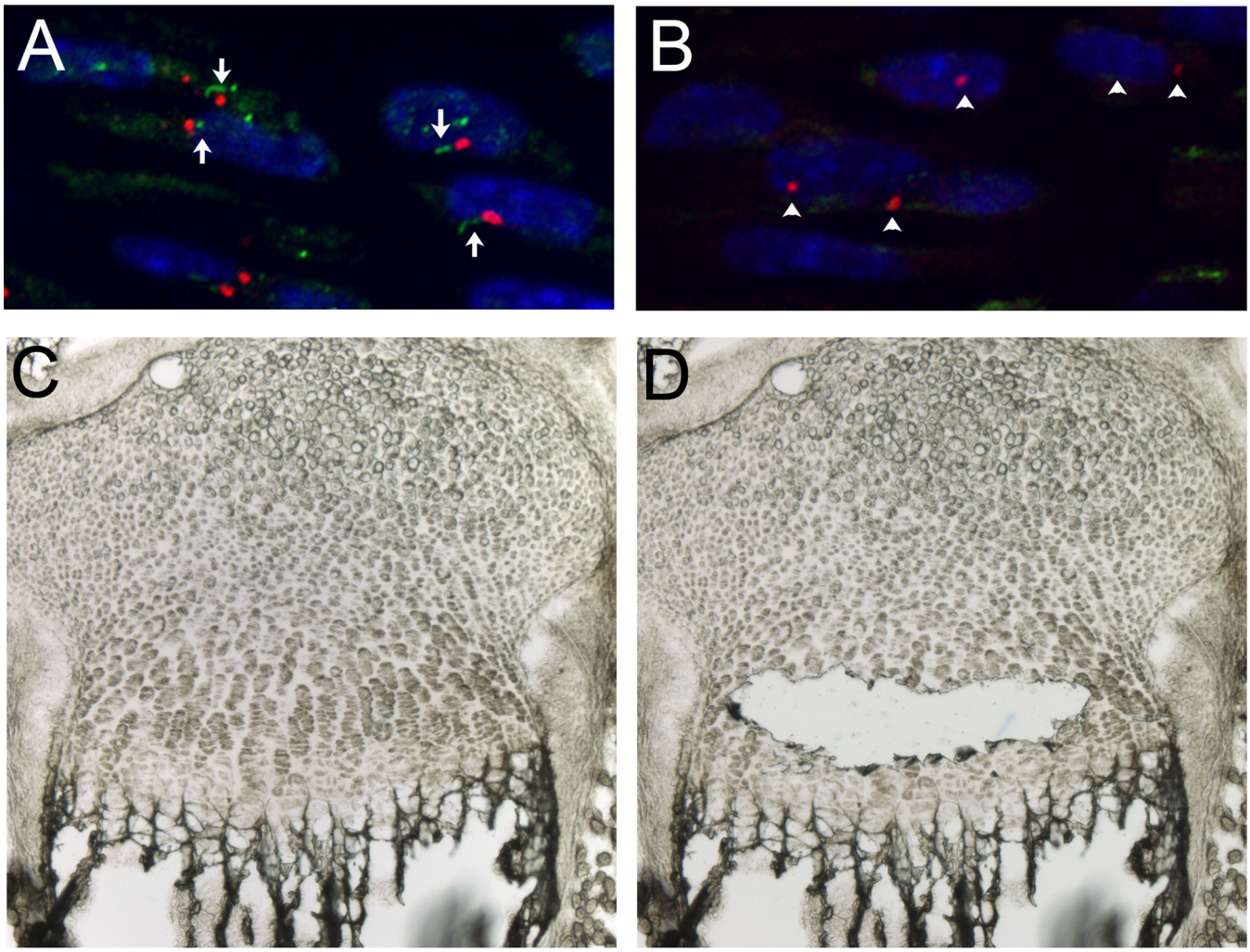

Figure 1. Micro-dissection of postnatal day 7 growth plate

Depletion of primary cilia was confirmed by immunostaining in growth plates from P7 control (A) and *Col2aCre;Ift88*$^{fl/fl}$ (B) mice. Ciliary bodies were stained with anti-Arl13b antibody (green), and the basal bodies were stained with anti-γ-tubulin antibody (red). The nuclei were stained with DAPI (blue). Images showing the cartilage tissue section on microscope slide before (C) and after (D) micro-dissection.

A

Gene	mutant/ control	Standard Error	P (H1)	Result
Axin2	1.439	1.115 - 1.853	0.004	up
Lef1	1.998	1.229 - 3.211	0.000	up

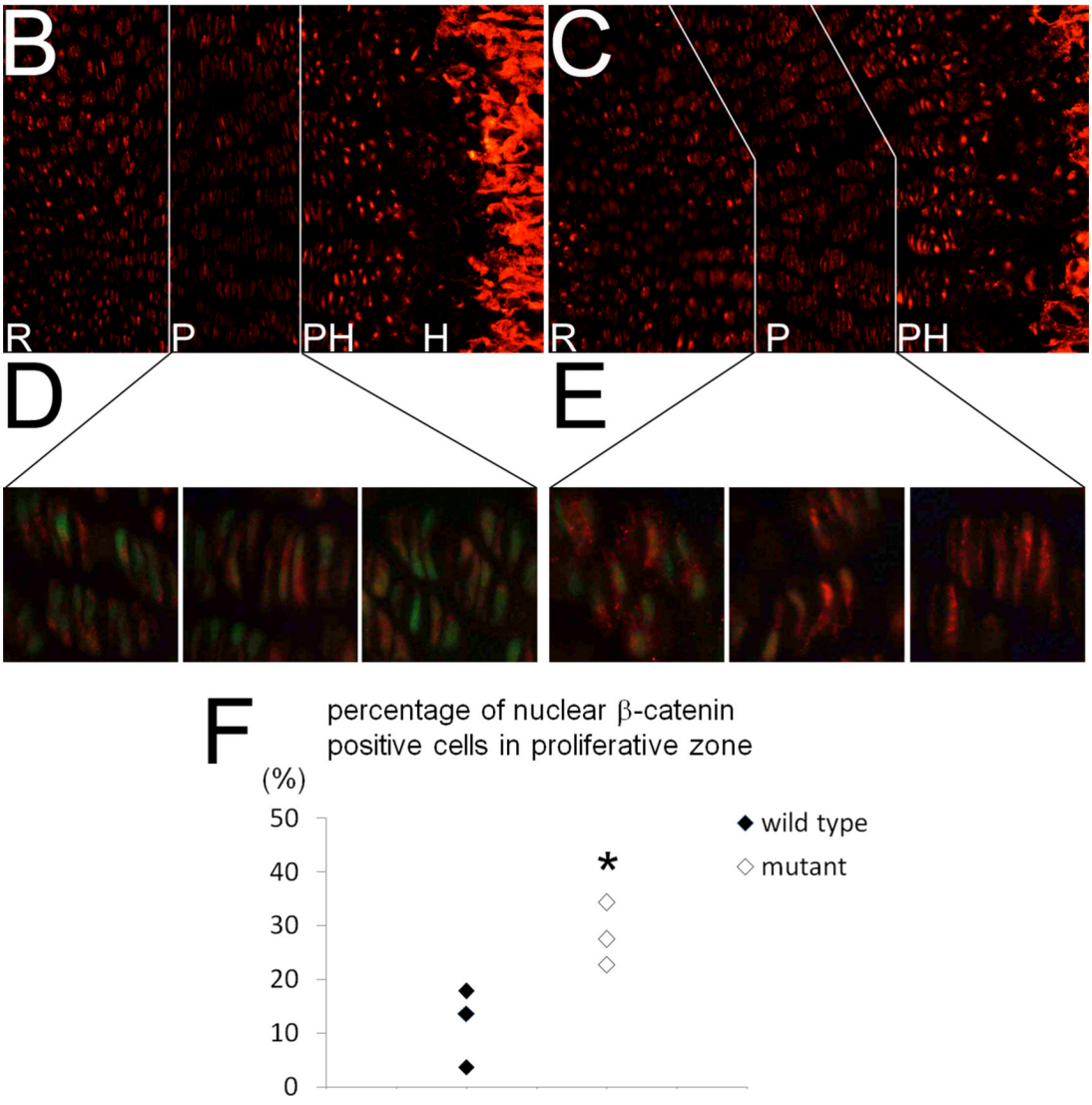

Figure 2. Canonical Wnt signaling in *Col2aCre;Ift88*$^{fl/fl}$ mutant cartilage

(A) Expression levels of *Axin2* and *Lef1* were measured by quantitative real time RT-PCR using RNA from micro-dissected columnar growth plate chondrocytes. Three separate control and mutant mice were used. Data was analyzed by REST software. *B2m* was used for normalization. (B-E) Immunostaining for β-catenin (red) in sections from the distal femur in control (B, D) and mutant (C, E) mice (10X magnification). High magnification images (D, E; 40X) demonstrating nuclear versus cytoplasmic staining in flat columnar chondrocytes for three random fields in sections from control (D) and mutant (E) mice. Nuclei are stained green with YoPro. (F) Three separate control and mutant samples were used to count nuclear β-catenin staining. Ten to fifteen columns in columnar chondrocytes

of the growth plate were counted for each sample (100–200 cells) and the percentage of cells with nuclear β-catenin staining was calculated as nuclear staining over total nuclei stained with YoPro in the field. Each point represents data from an individual mouse. The percentage of nuclear β-catenin was increased in mutant growth plate (χ-squared test, *$p<0.05$).

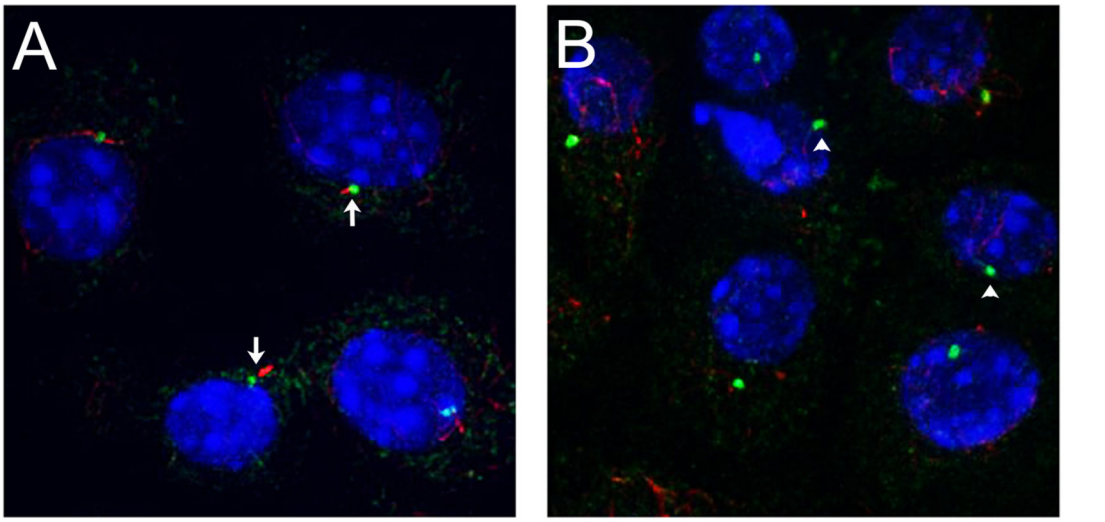

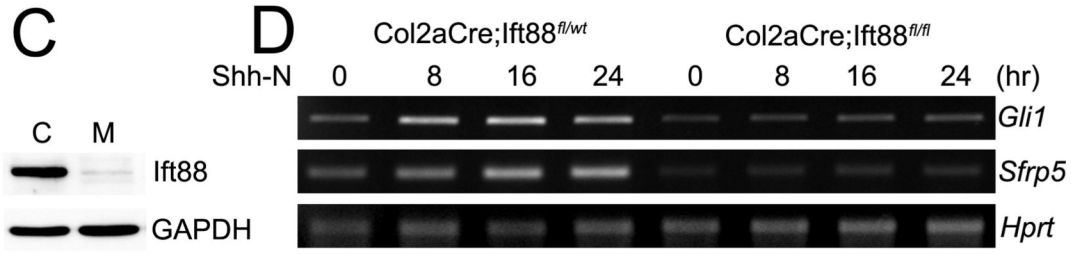

E

Gene	mut/con	Std. Error	P value	Result
Gli1	0.299	0.105 - 0.909	0.013	DOWN
Sfrp5	0.152	0.075 - 0.309	0.000	DOWN

F

0.5 μg/mL Shh-N	Col2aCre; Ift88fl/wt*			Col2aCre;Ift88fl/fl**		
	8h	16h	24h	8h	16h	24h
Gli1	1.749 (1.5-1.9)	1.932 (1.7-2.1)	2.915 (2.6-3.3)	1.077 (1.0-1.2)	1.146 (1.0-1.3)	2.014 (1.8-2.2)
Sfrp5	1.206 (1.1-1.3)	2.028 (1.9-2.2)	3.498 (3.1-3.9)	1.117 (1.0-1.3)	1.079 (0.9-1.2)	1.866 (1.7-2.0)

*treated/untreated control (Std. Error) **treated/untreated mutant (Std. Error)

Figure 3. *Gli1* and *Sfrp5* expression in Shh-N treated rib chondrocytes

Deletion of primary cilia was confirmed by immunostaining using anti-acetylated tubulin (red) and anti-γ-tubulin antibodies (green) in control (A) and mutant (B) cells. (C) Ift88 protein levels in control (c) and mutant (m) cells as measured by western blot. (D) Semi-quantitative RT-PCR measuring relative levels of Gli1 and Sfrp5 in control (*Col2aCre;Ift88*$^{fl/wt}$) and mutant (*Col2aCre;Ift88*$^{fl/fl}$) cells treated with 0.5μg/ml Shh-N for varying times (hr). Hprt was used as a loading control. (E) Real time RT-PCR comparing relative expression of Gli1 and Sfrp5 in untreated control and mutant cells. (F) Real time RT-PCR comparing untreated control cells to control cells treated with Shh-N for varying times and untreated mutant cells to mutant cells treated with Shh-N for varying times. RT-

PCR data was analyzed using REST software, expression levels of treated/ untreated samples with the standard error are shown. A representative of two separate experiments is shown. Each sample was analyzed in triplicate with Hprt used for normalization.

Table 1

Genes down-regulated (T-test p value < 0.05, >2-fold change) in proliferative zone of mutant growth plate.

Probe Set ID	Fold change down	Gene Symbol	Gene Title
1436838_x_at	2.010	Cotl1	coactosin-like 1 (Dictyostelium)
1416142_at	2.055	Rps6	ribosomal protein S6
1424308_at	2.079	Slc24a3	solute carrier family 24 (sodium/potassium/calcium exchanger), member 3
1417464_at	2.110	Tnnc2	troponin C2, fast
1427356_at	2.119	Fam89a	family with sequence similarity 89, member A
1420911_a_at	2.135	Mfge8	milk fat globule-EGF factor 8 protein
1438968_x_at	2.198	Spint2	serine protease inhibitor, Kunitz type 2
1417069_a_at	2.223	Gmfb	glia maturation factor, beta
1457111_at	2.229	AA415038	expressed sequence AA415038
1426565_at	2.248	Igf1r	insulin-like growth factor I receptor
1435338_at	2.371	Cdk6	cyclin-dependent kinase 6
1438936_s_at	2.627	Ang	angiogenin, ribonuclease, RNase A family, 5
1417868_a_at	2.992	Ctsz	cathepsin Z
1443837_x_at	3.033	Bcl2	B-cell leukemia/lymphoma 2
1427247_at	3.122	D3Bwg0562e	DNA segment, Chr 3, Brigham & Women's Genetics 0562 expressed
1419379_x_at	3.219	Fxyd2	FXYD domain-containing ion transport regulator 2
1434677_at	3.253	Hps5	Hermansky-Pudlak syndrome 5 homolog (human)
1416321_s_at	3.289	Prelp	proline arginine-rich end leucine-rich repeat
1416022_at	3.773	Fabp5	fatty acid binding protein 5, epidermal
1424196_at	4.028	Yipf1	Yip1 domain family, member 1
1435554_at	4.418	Tmcc3	transmembrane and coiled coil domains 3
1428853_at	4.425	Ptch1	patched homolog 1
1451814_a_at	5.275	Htatip2	HIV-1 tat interactive protein 2, homolog (human)
1436075_at	5.850	Sfrp5	secreted frizzled-related sequence protein 5
1443686_at	6.104	H2-DMb2	histocompatibility 2, class II, locus Mb2
1449058_at	6.155	Gli1	GLI-Kruppel family member GLI1
1436964_at	6.239	D7Ertd715e	DNA segment, Chr 7, ERATO Doi 715, expressed
1416889_at	9.012	Tnni2	troponin I, skeletal, fast 2

Table 2

Genes up-regulated (T-test p value < 0.05, >2-fold change) in proliferative zone of mutant growth plate.

Probe Set ID	Fold change up	Gene Symbol	Gene Title
1442489_at	2.016	D1Ertd564e	DNA segment, Chr 1, ERATO Doi 564, expressed
1439255_s_at	2.125	Gpr137b	G protein-coupled receptor 137B
1417814_at	2.130	Pla2g5	phospholipase A2, group V
1452382_at	2.168	Dnm3os	dynamin 3, opposite strand
1460453_at	2.243	Tagap1	similar to T-cell activation Rho GTPase-activating protein
1434667_at	2.271	Col8a2	collagen, type VIII, alpha 2
1437506_at	2.274	Adamts6	a disintegrin-like and metallopeptidase (reprolysin type) with thrombospondin type 1 motif, 6
1437128_a_at	2.293	A630033E08Rik	RIKEN cDNA A630033E08 gene
1421861_at	2.329	Clstn1	calsyntenin 1
1438441_at	2.330	Id4	Inhibitor of DNA binding 4 (Id4), mRNA
1426818_at	2.346	Arrdc4	arrestin domain containing 4
1426774_at	2.379	Parp12	poly (ADP-ribose) polymerase family, member 12
1448201_at	2.544	Sfrp2	secreted frizzled-related protein 2
1458667_at	2.643	4930519N13Rik	RIKEN cDNA 4930519N13 gene
1426518_at	2.672	Tubgcp5	tubulin, gamma complex associated protein 5
1459860_x_at	2.693	Trim2	tripartite motif-containing 2
1438878_at	3.220	6430537K16Rik	RIKEN cDNA 6430537K16 gene
1453152_at	3.504	Mamdc2	MAM domain containing 2
1435290_x_at	6.859	H2-Aa	histocompatibility 2, class II antigen A, alpha
1447360_at	14.370	Tsc22d1	TSC22-related inducible leucine zipper 1b (Tilz1b)

Table 3

Selected genes verified by real time RT-PCR.

Gene	Expression mutant/control	Standard Error	P value	Result
Gli1	0.271	0.197 – 0.374	0.000	DOWN
Ptch1	0.274	0.213 – 0.358	0.000	DOWN
Sfrp5	0.253	0.160 – 0.401	0.000	DOWN
Prelp	0.380	0.255 – 0.555	0.000	DOWN
Igf1r	0.714	0.531 – 0.995	0.005	DOWN
Bcl2	0.518	0.298 – 0.900	0.001	DOWN
Sfrp2	1.730	1.206 – 2.502	0.002	UP